# EEG-Based Pilot Emotion Monitoring Using KNN in Maneuvering Conditions

Arjon Turnip, Mohammad Taufik, Dwi Esti Kusumandari, and George Michael T.

Abstract—Flight safety is of paramount importance, and preventive measures are essential to maintain stable airline performance while minimizing accidents linked to pilots' emotional responses. This study investigates pilots' fear reactions during flight simulations using electroencephalography (EEG) signals and the K-Nearest Neighbors (KNN) algorithm, chosen for its simplicity and high classification accuracy of 94.08%. By analyzing brainwave patterns, this study highlights the connection between pilots' mental states, including attention levels at varying altitudes, and overall flight performance. The findings contribute to the aviation industry's efforts to enhance safety by understanding and mitigating emotional factors that could affect pilot decision-making.

Index Terms— Electroencephalography, Pilot, K-Nearest Neighbors.

# I. INTRODUCTION

PMODERN DEVELOPMENT presents several special challenges for pilots, one of which is altitude conditions that can cause various psychological reactions [1][2][3][4]. Detection and understanding of pilot altitude emotions is essential for improving flight systems because success in responding to and managing altitude emotions is critical to flight safety and performance [5][6]. The emotion of height, also known as aviophobia, can not only affect the overall performance of the pilot, but it can also cause extreme mental stress and tension [7][8]. In order to create effective intervention strategies and improve overall flight safety, it is essential to understand the emotional state of pilots [9][10].

Electroencephalogram (EEG) is one of the tests that can measure the electrical activity of the brain. In these situations, EEG can help understand how brain activity occurs during altitude [11]. EEG works to record and see the electrical amplitude of the brain with the placement of several electrodes on the human scalp. This understanding contributed to the creation of a useful high-altitude emotion detection system, which can track the emotional state of the pilo directly during flight [4][12].

In the medical world, the role of EEG has been widely used to diagnose disorders in the brain because EEG can read 5 brain

A. Turnip and M. Taufik, Department of Electrical Engineering, Universitas Padjadjaran, Sumedang, Indonesia (e-mails: turnip@unpad.ac.id, m.taufik@unpad.ac.id).

D. E. Kusumandari, National Research and Innovation Agency of Indonesia (BRIN), Indonesia (e-mail: dwie002@brin.go.id)

George Michael T., Precision Manufacturing System, Pusan National University, Republic of Korea (e-mail: georgetampubolon@pusan.ac.kr).

waves consisting of delta, theta, alpha, beta, and gamma [13]. The active conditions for each type of wave are different. When a person falls asleep soundly and without dreams, delta waves are active with a frequency of 0.5-4 Hz and an amplitude of 100-200 mV [14][15]. Theta waves are also active when very tired and close to sleep, with a frequency of 4-8 Hz and an amplitude of 5–10 mV [6][16][17]. When a person is calm or daydreaming, alpha waves are active with a frequency of 8–12 Hz and an amplitude of 20-80 mV. When a person is in a normal or fully conscious state, beta waves travel, with a frequency of 12-25 Hz and an amplitude of 1-5 mV. The last is Traveling gamma waves, with a frequency of 25-60 Hz and an amplitude of 0.5-2 mV [18][19]. There are other studies that aim to detect fatigue in car drivers and aircraft pilots using noninvasive methods [5]. However, the results of this test do not provide a quantitative synthesis of the findings, which may limit the robustness of the conclusions drawn [5][17].

This study aims to detect the emotional response of fear of heights to pilots with EEG signals, focusing on the use of the K-Nearest Neighbors (KNN) method as a classification tool. KNN was chosen for its simple nature, ability to handle high-dimensional datasets, and ability to provide good results in the context of classification. Through this research, it is hoped that a deeper understanding of the relationship between EEG signals and altitude emotions will be obtained, as well as the possible application of this technology in improving pilot safety and well-being. This research was carried out when the pilot was in a maneuvering position using 16 subjects that would be classified as fear levels.

### II. METHODOLOGY

This research was conducted in December 2022 and was conducted at Universitas Padjadjaran. In addition, we collaborated with the Indonesian Aviation Academy Banyuwangi to collect data for this study. The number of samples taken was 16 male and female samples. Subject data consisted of experienced and inexperienced individuals in flight at random. Before data collection, everyone involved in this study gave an explanation of the research objectives, processes, and procedures to be carried out.

During the study, to record the brain signals of the subjects, an EEG Mitsar 202 was used, and an electro cap was attached to the subject as well as an electro gel was applied to each EEG sensor to reduce the sound in the scalp in a relaxed state with the eyes open (Fig. 1a) [16]. There are 19 electrode channel channels, namely Fp1, Fp2, F7, F3, Fz, F4, F8, T3, C3,



Cz, C4, T4, T5, P3, Pz, P4, T6, O1, and O2[3].

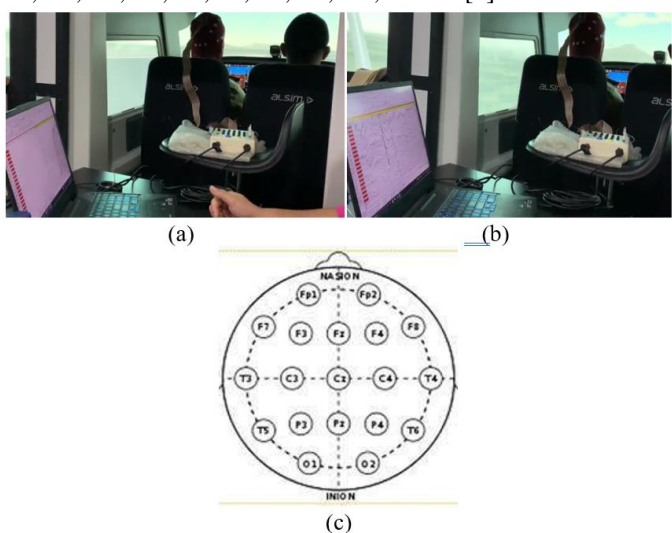


Fig. 1. (a)Electro-cap is attached to the subject (b) Subject in the maneuvering position (c) Placement of the electrode position on the human brain

Then after that the EEG signal data will be recorded and displayed using the WinEEG Visible Software in Fig. 2, which will then use a bandpass filter to display the recording results, reduce noise and eliminate unwanted frequencies. The low cutoff value is 0.3 (0.53 Hz) and the high cutoff value is 50 Hz.

The data recorded and processed with WinEEG are in the form of Delta, Theta, Alpha, Beta 1, Beta 2, and Gamma. After the data is processed with WinEEG, the phi V data unit is entered into Microsoft Excel. Thus, MATLAB software can process data with the classification learner feature, which then enters data from Microsoft Excel. Next, decide what method to use; In this study, the K-Nearest Neighbors method was used.

The K-Nearest Neighbors (KNN) method can be used to identify the emotional response of the pilot's altitude through the analysis of Electroencephalogram (EEG) signals. In this case, KNN functions as a classification algorithm that uses the principle that similar data tend to be in the same group. Using EEG signals, the KNN can find complex patterns that can indicate the emotional response of altitude in the pilot. EEG signals record the brain's electrical activity and changes in the frequency spectrum under various conditions, such as altitude. KNN works by measuring the distance between the data points to be predicted and the data points that are already in the exercise dataset. Therefore, KNN can account for patterns of brain activity in altitude situations similar to those that have been recorded in training data when analyzing EEG signals. The K value in KNN plays an important role, where the K value determines the number of nearest neighbors that will be used to predict the data class. In the detection of altitude emotions in pilots, choosing the right K value is essential to reduce noise and make more accurate predictions. This study seeks to simplify the difficulty of brain analysis during altitude situations by using KNN on EEG signals. A deeper understanding of EEG signal patterns allows this method to monitor and identify altitude emotions in pilots, which allows for the development of responsive and adaptive decision support systems in the world of aviation.

Geometric distance calculations, Hamming, Manhattan, and Minkowski are some of the types of distance calculations that can be used in KNN, depending on the nature of the data and the problem at hand. Choosing the right distance metric is crucial because it can affect the final outcome of the KNN algorithm. Calculating geometric distances can be done using the following equation:

$$Dxy = \sqrt{\sum_{i=1}^{n} (x_1 - y_1)^2}$$
 (1)

Hamming distance calculation can be done using the following equation:

$$Dxy = \frac{1}{n} \sum_{i=1}^{n} |x_i - y_i|$$
 (2)

Manhattan distance calculations can be done using the following equation:

$$Dxy = \sum_{i=1}^{n} |x_i - y_i| \tag{3}$$

Minkowski's distance calculation can be done using the following equation:

$$Dxy = \left(\sum_{i=1}^{n} |x_i - y_i|^p\right)^{\left(\frac{1}{p}\right)} \tag{4}$$

With the following information: Proximity distance (D) is a concept that measures the level of similarity between two cases, namely data training (x) and data testing (y). n reflects the number of individual attributes between 1 to n. The similarity function f describes the similarity of individual attributes (i) between cases X and Y, with i ranging from 1 to n.

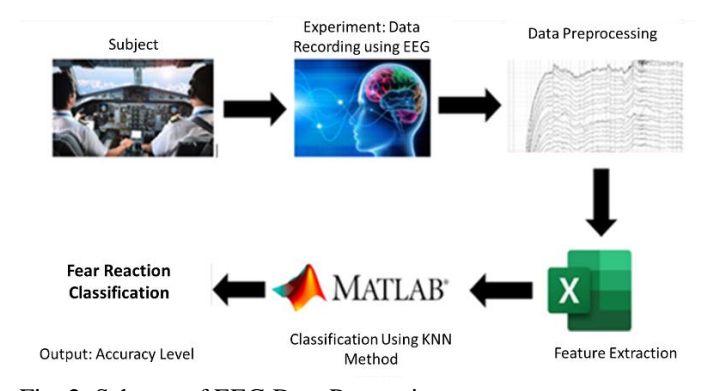


Fig. 2. Scheme of EEG Data Processing

### III. RESULTS AND DISCUSSION

The data that has been recorded has noise, a filtering process with a Band Pass Filter (BPF) is required with a range of 0.5 Hz to 50 Hz. Due to unnecessary signal cutting, the data stored is only necessary. The results of signal recording before and after the filtering process are compared in Fig. 3. Brain signals were obtained for three different conditions: the take-off condition, the maneuvering condition, and the landing condition. Therefore, the data is only taken from 85 - 155 seconds from the maneuver condition.

Once the EEG signal filtering is complete, the next stage is data extraction. At this stage, amplitude is used to capture data from three types of brainwave signals: alpha, beta 1 and beta 2. The EEG spectroscopy method is used to obtain this amplitude.

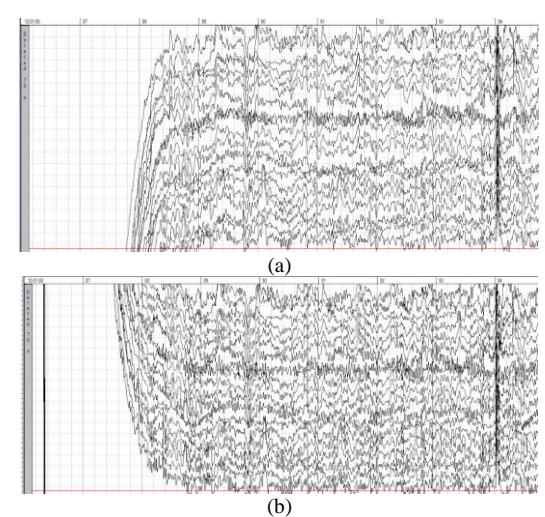


Fig. 3. Signal recording results (a) before (b) after cutting

Time intervals using fragments, using only EEG channels, epoch number 0, epoch length 1 second, overlapping none, time window Hanning, 3rd order polynomial trends, focus on slow waves with a signal power of 200, and a frequency range of 0.5 to 50 Hz. data without additional processing, and data alignment of 5 epochs. Fig.4. shows the data extracted in the form of brain mapping, graphs, and Table 1 shows the amplitude values of each electrode point. Brain Mapping shows where the electrode points are located and the active areas of the brain. The whiter the color, the more active the signal in the area.

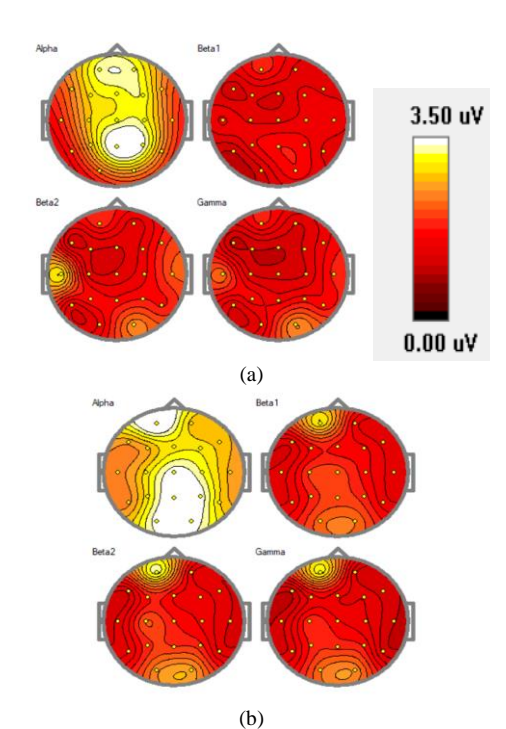


Fig. 4. The amplitude of the waves that have been extracted into the form of Brain Mapping (a) Inexperienced pilots (b) Experienced pilots

In Fig 5. read the condition of the subject when he is conscious, namely when flying. Then the data will be displayed

in the form of a graph which shows the amplitude value of each electrode point.

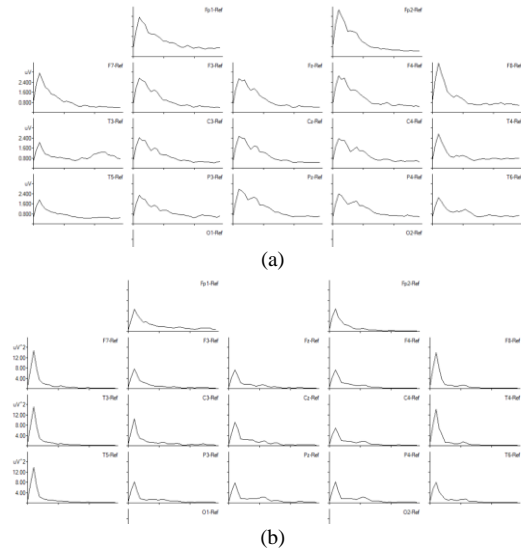


Fig. 5 The amplitude of the waves that have been extracted into the form of a graph (a) inexperienced pilots (b) experienced pilots

TABLE I

DATA RESULTS THAT HAVE BEEN EXTRACTED

Subject	Alpha	Betha 1	Betha 2	Gamma
Subject	2.243	1.586	1.734	1.664
Subject 2	2.542	1.944	2.450	2.437
Subject 3	2.040	1.373	1.334	1.563
Subject 4	1.454	0	1.065	1.078
Subject 5	3.083	1.633	1.864	1.605
Subject 6	2.136	1.230	1.430	1.257
Subject 7	2.080	1.496	1.610	1.479
Subject 8	1.933	1.370	1.506	1.497
Subject 9	1.551	0	0	0
Subject 10	1.914	1.362	1.399	1.522
Subject 11	2.990	1.747	1.729	1.541
Subject 12	0	0	0	0
Subject 13	1.961	1.379	1.465	1.342
Subject 14	2.355	1.631	1.695	1.649
Subject 15	2.355	1.631	1.695	1.649
Subject 16	2.611	1.827	1.838	3.921



There are 304 data from 16 subjects that will be classified into 5 categories and then filter, normalize and extract data from the 16 subjects and determine the maximum, minimum, range, and interval values in Table 2.

TABLE II
RESULTS OF MAXIMUM, MINIMUM, RANGE AND INTERVAL VALUES

Maximum Value	30.295
Minimum Values	0
Range	30.295
Interval	6.059

To determine the interval in the data classification, the maximum and minimum values that have been obtained are used. After that the data is normalized, the amplitude comes from the waves (Alpha, beta 1, beta 2, gamma) to get the total at each electrode location. The next step is grouped into 5 categories, namely strongly Acrophobia, Active Acrophobia, Moderate Acrophobia, Low Acrophobia, and None Acrophobia. The results of the classification based on intervals are as follows: In the Acrophobia classification, the amplitude interval (uV) is used as a parameter. There are five categories with different amplitude ranges, namely Strongly Acrophobia (24,236 - 30,295 uV), Active Acrophobia (18,277 - 24,236 uV), Moderate Acrophobia (12,118 - 18,177 uV), Low Acrophobia (6059 - 12,118 uV), and No Acrophobia (0 - 6059 uV).

Furthermore, the data is used for classification learning in Matlab. To determine the level of accuracy, the KNN technique is used in this classification process. In this experiment, the authors conducted data training for each type of KNN method, which resulted in varying levels of accuracy in Table 3. The Weighted method is the most accurate and fast of all KKN models, with an accuracy of 94.08% and a prediction speed of 1800 observations per second.

TABLE III TRAINING RESULT METODE KNN

Model type	Accurac y	total cost	Prediction Alert(obs/s ec)	Training Time (sec)
Fine KNN	93.09%	21	1800	14.667
Medium KNN	89.80%	31	1700	11.083
Coarse KNN	80.92%	58	1600	10.646
Cosine KNN	81.25%	57	1700	9.329
Cubic KNN	88.16%	36	1700	14.737
Weighted KNN	94.08%	18	1800	14.667

The researcher uses the KNN method to process normalized extraction data, presenting it through various forms of data representation. The results of the test through the simulation

show that the Weighted KNN method has the highest level of accuracy compared to the other five methods, reaching 94.08%. This method uses a variety of plots, such as dispersion plots, confusion matrix plots, and parallel coordinate plots. The high-test results of the Weighted KNN plot show that this method is effective in processing and analyzing data correctly.

In a scatter plot, the dots show the data for two numerical variables. In the context of model predictions, a scatter plot is used to visualize the model's performance by plotting predicted values against actual values. Each point on the plot represents a prediction made by the model. Dots (•) indicate correct predictions, while crosses (X) represent incorrect ones. As shown in Fig. 6, only a few incorrect predictions were made. The confusion matrix, which consists of four combinations of actual and predicted values, can also be used to assess the performance of the model. In combination this includes the Original Positive Value (TPR), which is the true positive proportion of all predicted positive samples; False Negative Value (FNR), which is the proportion of false negatives; Positive Prediction Value (PPV), which indicates the accuracy between the prediction and the actual classification; and False Discovery Value (FDR). The confusion matrix shows how well the model can correctly classify the data and find positive and negative cases precisely. We can evaluate the strengths and weaknesses of the model in predicting and classifying data by examining the combination of TPR, FNR, PPV, and FDR values.

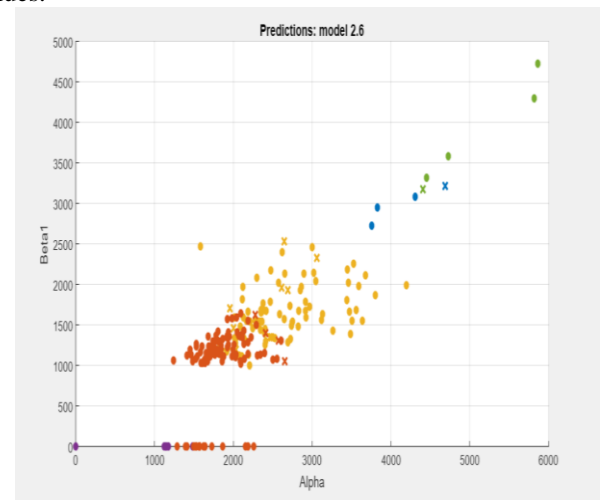


Fig. 6. Scatter Plot: dot (●) is correct and cross (X) is incorrect predictions.

In this analysis, the False Negative Rate (FNR) for the confusion matrix in Fig. 7 stands out, with the highest value being 57.1%. This indicates that a significant portion of true positives were misclassified as negatives, highlighting a key area for improvement in the model's performance. Looking into the individual categories, the True Positive Rate (TPR) for the Strongly Acrophobic category was relatively high at 83.3%, meaning that the model was able to correctly classify the majority of instances in this category. However, this also suggests that there is room for improvement, given the elevated FNR of 16.7%. For the Acrophobia Note category, the model performed exceptionally well, achieving a TPR of 98.8%,

signifying that nearly all instances in this category were accurately identified. Additionally, the FNR for this category was remarkably low at 1.2%, which demonstrates a high level of precision and reliability in distinguishing this level of acrophobia. Similarly, for the Moderate Acrophobia category, the TPR was also high at 95.1%, with an FNR of 4.9%. These values indicate that the model effectively identifies cases in this category, though a slight reduction in misclassification would further strengthen its performance.

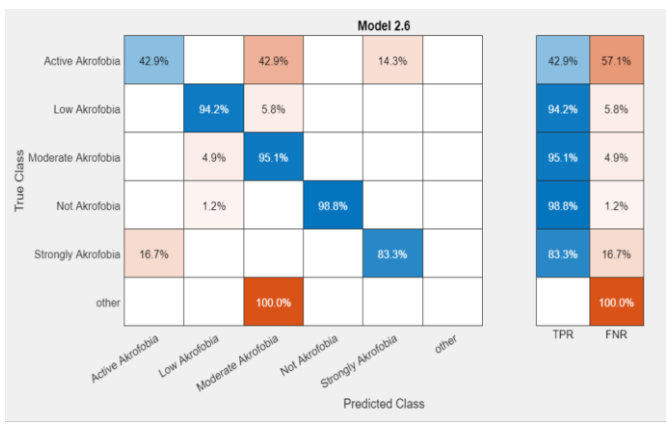


Fig. 7. Confusion matrix TPR dan FNR.

In Fig. 8, the confusion matrix illustrates the performance of the model through the Positive Predictive Value (PPV) and False Discovery Rate (FDR) across different categories related to acrophobia levels: Not, Low, Moderate, Active, and Strongly Acrophobic. The PPV, which indicates the proportion of correctly identified positives, shows a range from 75% to 100% across the categories. This variation in PPV reflects the model's effectiveness in distinguishing between different levels of acrophobia. Specifically, the Not acrophobic category achieved a PPV of 75%, indicating a moderate level of accuracy in identifying individuals with no acrophobia. The Low and Moderate categories show significantly higher PPV values of 94.2% and 90.7%, respectively, highlighting strong model performance in detecting these levels of acrophobia.



Fig. 8. Confusion matrix PPV dan FDR.

The Active acrophobia category had a perfect PPV of 100%, demonstrating the model's complete accuracy in identifying this group without any false positives. However, for the Strongly Acrophobic category, the PPV dropped slightly to 83.3%, indicating some degree of misclassification, though still maintaining a relatively high accuracy. The PPV for the Other category is notably lower at 0.9%, signaling poor classification performance in this group. This could suggest that the model struggles to differentiate the Other category from the defined acrophobia levels, likely due to overlapping or ambiguous characteristics within this category. Overall, the PPV results suggest that the model is highly effective at classifying common acrophobia categories, with minor misclassifications in the more extreme cases (Strongly Acrophobic) and significant difficulties with the Other category. This suggests that further refinement is needed, especially to handle outliers or less clearly defined categories.

Parallel coordinate plots are useful for analyzing multivariate numerical data. Comparison between samples or observations on various numerical variables is made easier with this graph. Different axes denote each feature or variable, and each axis is parallel to each other and at the same distance. This method allows researchers to easily find patterns or relationships between numerical variables. This allows them to do this without projecting data to a lower dimension. By using parallel coordinate plots, data complexity can be deciphered and understanding of patterns that may be hidden in variable relationships can be improved.

Fig. 9 is the parallel coordinate plot of prediction model: Solid line (---) and Dash line (---) are correct and incorrect predictions, respectively. The lines in the figure represent the class for each variable, where Green corresponds to the Strongly Acrophobic class, Purple represents Not Acrophobic, Orange indicates Moderate Acrophobia, Red signifies Low Acrophobia, and Blue denotes Active Acrophobia. The solid lines indicate that the model accurately predicted the output for the selected features, while the dashed lines highlight less accurate predictions. Overall, the results in Fig. 9 demonstrate that only a few predictions were classified inaccurately, which aligns with the model's high accuracy of 94%. Notably, the majority of prediction errors were observed in the Moderate Acrophobia class. This could suggest that the features for this class overlap or are less distinct compared to other classes, making it more challenging for the model to differentiate. However, given the overall accuracy, the model still performs well across most categories, with minimal misclassification.

A line diagram connecting the subject's reference values can effectively describe parallel algorithms in the following data representations. Furthermore, by using standard deviations displayed on parallel charts, clear and prominent visual representations are created. This makes the interpretation of results more intuitive. K-Nearest Neighbors (KNN), a versatile machine learning method for both classification and regression, is particularly effective for monitoring drones and analyzing the data they generate. By using a distance-based approach, KNN classifies observations based on the majority of their nearest neighbors, enabling more accurate monitoring and analysis. This method enhances the understanding of patterns and relationships within the data, providing deeper insights.



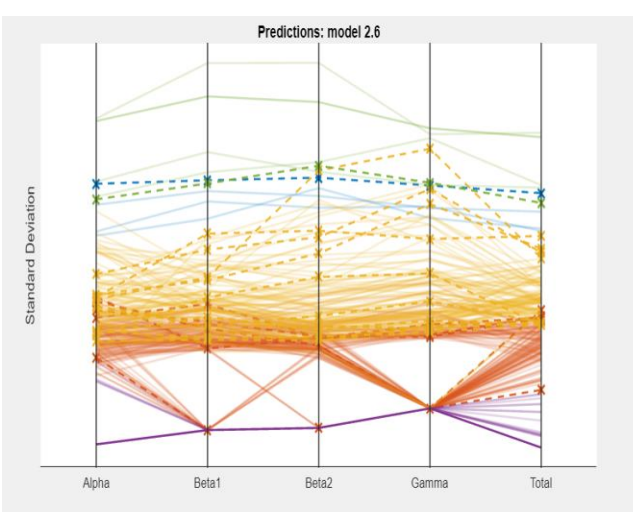


Fig. 9. Parallel Coordinate Plot of prediction model: Solid line (—) and Dash line (—) are correct and incorrect predictions, respectively. (Lines: Green: Strongly, Purple is Not, Orange is Moderate, Red is Low, Blue is Active)

### IV. CONCLUSION

The study examines the emotional categorization of pilots based on altitude-related acrophobia using EEG signals and the K-Nearest Neighbor (KNN) algorithm. Sixteen pilots participated in flight simulations where brainwave patterns—specifically alpha, beta 1, beta 2, and gamma waves—were recorded and analyzed. After a thorough process of EEG data filtration and feature extraction, the KNN model achieved an impressive accuracy of 94.08%. From a total of 304 data points, the emotional responses were classified into four categories: strong acrophobia, active acrophobia, low acrophobia, and no acrophobia. The results highlight the effectiveness of this method in detecting fear responses through EEG signals with a high degree of precision.

## ACKNOWLEDGMENT

This research was supported by the Department of Electrical Engineering, *Universitas Padjadjaran*, Bandung, Indonesia and the *Akademi Penerbangan Indonesia*, Indonesia.

# REFERENCE

- [1] V. Zotev and J. Bodurka, "Effects of simultaneous real-time fMRI and EEG neurofeedback in major depressive disorder evaluated with brain electromagnetic tomography," *NeuroImage: Clinical*, vol. 28, 2020. doi: 10.1016/j.nicl.2020.102459.
- [2] D. Acharya, A. Billimoria, N. Srivastava, S. Goel, and A. Bhardwaj, "Emotion recognition using Fourier transform and genetic programming," *Applied Acoustics*, vol. 164, 2020. doi: 10.1016/j.apacoust.2020.107260.
- [3] E. Q. Wu, P. Y. Deng, X. Y. Qiu, Z. Tang, W. M. Zhang, L. M. Zhu, H. Ren, G. R. Zhou, and R. S. F. Sheng, "Detecting fatigue status of pilots based on deep learning network using EEG signals," *IEEE Transactions on Cognitive and Developmental Systems*, vol. 13, no. 3, pp. 575–585, 2021. doi: 10.1109/TCDS.2019.2963476.
- [4] F. Saffari, K. Norouzi, L. E. Bruni, S. Zarei, and T. Z. Ramsøy, "Impact of varying levels of mental stress on phase information of EEG signals: A study on the frontal, central, and parietal regions," *Biomedical Signal Processing and Control*, vol. 86, 2023. doi: 10.1016/j.bspc.2023.105236.
- [5] X. Hu and G. Lodewijks, "Detecting fatigue in car drivers and aircraft pilots by using non-invasive measures: The value of differentiation of

- sleepiness and mental fatigue," *Journal of Safety Research*, vol. 72, pp. 173–187, 2020. doi: 10.1016/j.jsr.2019.12.015.
- [6] L. Wang, S. Gao, R. Hong, and Y. Jiang, "Effects of age and flight exposure on flight safety performance: Evidence from a large crosssectional pilot sample," *Safety Science*, vol. 165, 2023. doi: 10.1016/j.ssci.2023.106199.
- [7] R. Ghosh, N. Deb, K. Sengupta, A. Phukan, N. Choudhury, S. Kashyap, S. Phadikar, R. Saha, P. Das, N. Sinha, and P. Dutta, "SAM 40: Dataset of 40 subject EEG recordings to monitor the induced-stress while performing Stroop color-word test, arithmetic task, and mirror image recognition task," *Data in Brief*, vol. 40, 2022. doi: 10.1016/j.dib.2021.107772.
- [8] A. Turnip, et al., "Detection of Drug Effects on Brain-Based EEG Signals using K-Nearest Neighbours," 2023 IEEE 9th Information Technology International Seminar (ITIS), IEEE, 2023.
- [9] Tran, Minh Anh, et al. "EEG-Based Emotion Feature Extraction Using Power Spectral Density." 2023 15th International Conference on Knowledge and Systems Engineering (KSE), IEEE, 2023.
- [10] Aderinwale, G. B. Tolossa, A. Y. Kim, E. H. Jang, Y. il Lee, H. J. Jeon, H. Kim, H. Y. Yu, and J. Jeong, "Two-channel EEG based diagnosis of panic disorder and major depressive disorder using machine learning and non-linear dynamical methods," *Psychiatry Research - Neuroimaging*, vol. 332, 2023. doi: 10.1016/j.pscychresns.2023.111641.
- [11] G. Vanhollebeke, S. De Smet, R. De Raedt, C. Baeken, P. van Mierlo, and M. A. Vanderhasselt, "The neural correlates of psychosocial stress: A systematic review and meta-analysis of spectral analysis EEG studies," *Neurobiology of Stress*, vol. 18, 2022. doi: 10.1016/j.ynstr.2022.100452.
- [12] M. F. J. Sperl, A. Wroblewski, M. Mueller, B. Straube, and E. M. Mueller, "Learning dynamics of electrophysiological brain signals during human fear conditioning," *NeuroImage*, vol. 226, 2021. doi: 10.1016/j.neuroimage.2020.117569.
- [13] E. Perez-Valero, M. A. Lopez-Gordo, and M. A. Vaquero-Blasco, "EEG-based multi-level stress classification with and without smoothing filter," *Biomedical Signal Processing and Control*, vol. 69, 2021. doi: 10.1016/j.bspc.2021.102881.
- [14] A. Turnip et al, "Pilot Fear Detection from EEG Signals Classified by Decision Tree During Landing Conditions," 2024 IEEE International Conference on Artificial Intelligence and Mechatronics Systems (AIMS), 2024
- [15] R. M. Mehmood, M. Bilal, S. Vimal, and S. W. Lee, "EEG-based affective state recognition from human brain signals by using Hjorthactivity," *Measurement: Journal of the International Measurement Confederation*, vol. 202, 2022. doi: 10.1016/j.measurement.2022.111738.
- [16] A. Turnip et al, "Comparison of Classification Systems for Detection of Drug Effects on the Brain Using Machine Learning-Based EEG Signals," 2024 IEEE International Conference on Artificial Intelligence and Mechatronics Systems (AIMS), 2024.
- [17] P. Kouba, M. Šmotek, T. Tichý, and J. Kopřivová, "Detection of air traffic controllers' fatigue using voice analysis - An EEG validation study," *International Journal of Industrial Ergonomics*, vol. 95, 2023. doi: 10.1016/j.ergon.2023.103442.
- [18] M. K, P. S, A. K, R. D, V. Chinnadurai, V. S, R. K, and S. Jayaraman, "Dynamic cognitive workload assessment for fighter pilots in simulated fighter aircraft environment using EEG," *Biomedical Signal Processing* and Control, vol. 61, 2020. doi: 10.1016/j.bspc.2020.102018.
- [19] R. Agarwal, M. Andujar, and S. Canavan, "Classification of emotions using EEG activity associated with different areas of the brain," *Pattern Recognition Letters*, vol. 162, pp. 71–80, 2022. doi: 10.1016/j.patrec.2022.08.018.
- [20] D.-H. Lee, J.-H. Jeong, K. Kim, B.-W. Yu, and S.-W. Lee, "Continuous EEG decoding of pilots' mental states using multiple feature block-based convolutional neural network," *IEEE Access*, vol. 8, pp. 121929-121941, 2020. doi: 10.1109/ACCESS.2020.3005647.
- [21] H. Choubey and A. Pandey, "A combination of statistical parameters for the detection of epilepsy and EEG classification using ANN and KNN classifier," Signal, Image and Video Processing, vol. 15, no. 3, pp. 475– 483, 2021. doi: 10.1007/s11760-020-01767-4.
- [22] V. Doma and M. Pirouz, "A comparative analysis of machine learning methods for emotion recognition using EEG and peripheral physiological signals," *Journal of Big Data*, vol. 7, no. 1, 2020. doi: 10.1186/s40537-020-00289-7.